Cutting Performance and Microstructure of High Speed Steels: Contributions of Matrix Strengthening and Undissolved Carbides

S. KARAGÖZ and H.F. FISCHMEISTER

While it is accepted that both the hot strength of the matrix and the amount of undissolved carbides are important for the cutting performance of high speed steels, the relative weights of their contributions are unknown. In this work, they are separately identified and a model is presented that provides a quantitative prediction of tool life (solely in uninterrupted cutting) on the basis of microstructural and compositional data over a wide range of alloy compositions and cutting speeds. The model seems to describe the individual contributions to tool life well enough to serve as a guide in alloy development. The model has been developed using 13 different steels, spanning the entire range of customary compositions. It is based on the following parameters: volume fractions and compositions of undissolved carbides; precipitates formed during tempering (secondary hardening) and during operation (tertiary precipitates); and, finally, residual solute in the matrix. Tool life is modeled as a linear combination of contributions from the undissolved carbides and from the precipitate population, including a contribution due to the action of Co, and with an additional term due to solute strengthening of the matrix. The weight factors are determined by multiple linear regression analysis. They reflect the relative importance of each contributing factor, and their dependence on cutting speed can be interpreted in terms of the change in operative wear mechanism with tool temperature.

I. INTRODUCTION

THE alloy compositions and microstructures of today's high speed steels are the result of decades of empirical development.[1,2,3] Alloy profiles are customarily described in the dimensions of wear resistance, hot strength, and toughness. This article deals with two of these, hot strength and wear resistance, trying to assess their relative contributions to tool life in uninterrupted cutting, and to establish quantitative relations with microstructural features.

Toughness, while important in intermittent cutting, is a secondary concern in uninterrupted chip forming. Therefore, we will merely outline our philosophy. Although the relevant property is actually the resistance to edge chipping,[4–7] the tool materials community prefers to characterize toughness by the more easily measured rupture strength. This property can be understood[4,6,8] in terms of the size distribution of crack initiating defects or inhomogeneities[5,6,8] and of the material's crack propagation resistance. The latter is fairly constant in the relevant state of heat treatment, varying little with alloy composition and microstructure.[4,5,9] Thus, ''toughness'' in the sense of rupture strength mainly reflects the defect population, which is a function of cleanliness and processing rather than alloy composition.

Wear resistance in high speed steels is customarily associated with a population of carbide particles in the micrometer size range, down to several tenths of a micrometer, which have survived the austenitization treatment without going into solution.[6,10–13] They are embedded in a matrix of tempered martensite, which derives its strength from very fine (nanometer-sized) carbides precipitated during tempering in a process known as secondary hardening.[14–23] We will refer to the two populations as undissolved (or blocky) carbides and secondary precipitates, respectively. The blocky carbides are too coarse to strengthen the material other than by the load transfer mechanism which acts in particle composites; their main role is to protect the material from abrasive and adhesive wear.[23]

Hot strength is important in two respects: the matrix must be strong enough at operating temperature to prevent plucking of undissolved carbides from the contact surface and to resist plastic blunting.[24,25] It has been demonstrated[23] that the secondary hardening of the matrix can be accounted for in terms of Orowan strengthening with pertinent precipitate spacings. The compositions, types, and sizes of the secondary precipitates have been studied by field ion microscopy combined with the atom probe technique (APFIM),[21,22,26] and it has been shown that the loss of strength through precipitate coarsening at operating temperatures is compensated, to some degree, by the formation of further, ''tertiary'' precipitates.[26] The customary tempering treatments transform merely about half the solute in the oversaturated matrix into precipitates.[22] The remainder forms a reservoir for tertiary precipitation during operation.[26] When carbon is the limiting component for this, a certain amount of metallic elements remains in solution, providing a last defense by solute strengthening.

Wear mechanisms in high speed steels have been reviewed by Wright and Trent,[27] Söderberg *et al.*,[28,29] and

S. KARAGÖZ, formerly on leave at the Max-Planck-Institut für Metallforschung, D-70174 Stuttgart, Germany, is Professor of Metallurgy and Head of the Department of Metallurgy, Kocaeli University, TR-41040 Izmit, Turkey. H.F. FISCHMEISTER, FASM, formerly Professor of Metallurgy, University of Stuttgart, and Director, Max-Planck-Institut für Metallforschung, is retired. Present address: Department of Materials Engineering and Welding, Technical University, Graz, A-8010 Graz (Austria).

Manuscript submitted May 28, 1997.

others.[30] Depending on the cutting conditions, on the work material, and on the site on the tool surface (flank or crater), different mechanisms predominate. In uninterrupted cutting, important mechanisms are adhesive wear, abrasive wear, and, ultimately, plastic blunting due to thermal softening, which is connected with precipitate coarsening. Interdiffusion between tool and work material may cause loss of carbon and dissolution of carbides from the tool into the chip. Strongly emphasized in early work,[31] this mechanism is now considered to be of importance mainly at high speeds on the flank face, where the tool surface is permanently in contact with virgin work material.[32] In the regime of low and intermediate cutting speeds, which comprises the main applications of high speed steels, adhering work material tends to form a built-up edge,[29,31] which protects the cutting edge from abrasion and, through the change in cutting geometry,[33] also from thermal softening in a limited degree. Microcracking induced by thermomechanical fatigue and edge chipping is important in operations where tool/work contact is intermittent,[28] but not in uninterrupted cutting, which is our present subject.

The wear resistance of high speed steels has been found to increase with the volume fraction of undissolved carbides,[24,27–29,34] especially in operations where abrasion is dominant.[35] This is in agreement with the general trends of abrasion in metal-ceramic composites.[36] Large volume fractions of undissolved carbides have also proved beneficial with respect to plastic blunting, an effect ascribed to composite strengthening.[37]

Attempts to rank the performance of high speed steels merely on the basis of their content of undissolved carbides have, however, failed except within narrow groups of closely related alloys.[24,38] Other factors must play an important role, and those responsible for matrix strengthening would appear to be the prime candidates.

A positive correlation of tool life with tempered hardness is generally recognized.[24,29,35,39] Henderer[23] tried to correlate the performance of twist drills to alloy composition for a series of lean steels designed to keep the population of undissolved carbides as low as possible. Carbon and carbide formers were kept in stoichiometric balance, in accordance with the popular ''carbon saturation'' concept.[40,41] Linear regression analysis revealed a strong correlation of tool life with vanadium content, while the sensitivity to W, Mo, and C appeared to be weak within the (limited) range of variation. The positive influence of V was attributed to its importance for secondary precipitate formation, but undissolved carbides, which would also contribute to tool life, could not be avoided at higher V contents. The indistinct correlation of tool life with all alloy elements except V shows that a serviceable model for tool performance cannot be based merely on the alloy contents of individual elements. The structure of the model presented here is more complex, but also more deterministic, in that it takes into account the ways in which individual alloy elements affect the population of blocky carbides, on the one hand, and matrix strengthening, on the other.

In the early era of powder metallurgy processing of tool steels, great hopes were attached to controlling the size and spatial distributions of the undissolved carbides. It has come to be realized that the main effect of the finer carbide distribution is increased toughness, which allows the carbide content to be raised, thereby contributing indirectly to wear resistance.[42] This view is borne out by the present study, which includes both conventionally and powder processed materials.

Despite its largely intuitive basis and the absence of clear proof, the role assignment of hot strength to the precipitates, and wear resistance to the undissolved carbides, has become the general basis of the alloying philosophy for high speed steels. A classical example is the development of AISI M41, as described by Steven *et al.*[40] Roberts[2] tried to combine an independently optimized matrix with an optimized amount of undissolved MC carbides. With vanadium as the main MC former, the role separation did not succeed well: the high solubility of vanadium monocarbide in austenite makes for contributions to both blocky carbide formation and secondary precipitation. The concept is more easily realized with a stabler monocarbide such as NbC.[43]

The works quoted in this section diverge widely with respect to the relative weights ascribed to undissolved carbides and matrix strengthening. In the present article, we try to assess these contributions empirically. For a wide selection of high speed steels, volume fractions of undissolved carbides and the precipitation and solute strengthening of the matrix are correlated with tool lives by multiple linear regression analysis. The underlying hypothesis, that these factors (and no others) are indeed the salient factors determining tool life and that their effects combine additively without strong cross effects, is verified by the results.

II. EXPERIMENTAL

A. *Alloys*

Table I shows the compositions of the 13 alloys used in this study, the heat treatments applied, and the resultant hardness levels. The composition range comprises all of the classical alloy types, starting from the tungsten grade AISI T1 (no. 1) *via* the tungsten-molybdenum grade AISI M2 (no. 2) to the molybdenum-rich AISI M7 (no. 3). Number 4 (AISI M42) is a high-carbon derivative of M7; no. 5 is a high-carbon, high-vanadium derivative of M2 with addition of cobalt, and no. 6 is a cobalt-alloyed tungsten grade similar to AISI T15. Numbers 7 through 10 are experimental alloys with varying cobalt levels in a base composition in which vanadium has been partially replaced by niobium.[43,44] Finally, nos. 11 through 13 represent the matrices of T1, M2, and M7 without the blocky carbides. These ''carbide-free'' alloys were originally made for a field ion microscope study of tempering reactions.[22] Their wear data are included here to demonstrate the effect of blocky carbides by comparison with the parent alloys. The finer carbide distributions and higher carbon contents allowed by powder metallurgy processing are represented by nos. 5 through 10.

B. *Microstructure Characterization*

Typical micrographs will be shown in Section III (Figures 3 and 4). The volume fractions of undissolved carbides were measured on scanning electron micrographs taken with a JEOL* 6400 instrument and quantified with a Quan-

*JEOL is a trademark of Japan Electron Optics Ltd., Tokyo.

Table I. Alloy Compositions, Heat Treatment, and Hardness in the Finished, Heat-Treated State

Alloy Number	Alloy Type AISI	Alloy Type DIN	Chemical Composition (Wt Pct) C	W	Mo	V	Cr	Co	Nb	Austenitization (°C/3 min)	Tempering (°C/1 h)	Hardness (HRC)
1	T1	S18-0-1	0.74	17.86	0.41	1.02	3.81	—	—	1280	3 × 550	64.0
2a										1190	3 × 550	64.5
2b	M2	S6-5-2	0.92	5.99	4.50	1.55	3.77	—	—	1220	3 × 550	65.0
2c										1220	3 × 550	
											1 × 600	63.0
3	M7	S2-9-2	0.84	1.62	8.77	1.16	3.56	—	—	1190	3 × 550	64.5
4	M42	S2-9-1-8	1.09	1.22	8.78	1.02	3.67	7.71	—	1200	3 × 540	67.5
5	PM/M2mod.	S-6-5-4	1.30	5.55	4.26	3.70	3.69	—	—	1210	3 × 540	65.0
6	PM/T15mod.	S10-2-5-8	1.60	10.00	1.98	4.76	3.53	8.07	—	1210	3 × 540	67.0
7	PM/exp Nb		1.31	2.00	3.04	1.68	4.37	—	3.43	1230	3 × 560	64.5
8	PM/exp Nb + 3Co		1.28	2.22	3.00	1.64	4.30	3.64	3.44	1230	3 × 540	65.5
9	PM/exp Nb + 5Co		1.28	2.24	3.12	1.70	4.50	5.52	3.28	1230	3 × 540	66.0
10	PM/exp Nb + 8Co		1.26	2.12	2.96	1.56	4.20	8.36	3.44	1230	3 × 530	66.5
11	T1-Mx		0.44	7.29	0.55	0.69	4.11	—	—	1240	3 × 550	58.5
12	M2-Mx		0.55	3.93	3.57	0.99	4.63	—	—	1200	3 × 550	62.5
13	M7-Mx		0.52	1.12	4.58	1.03	4.00	—	—	1180	3 × 550	60.5

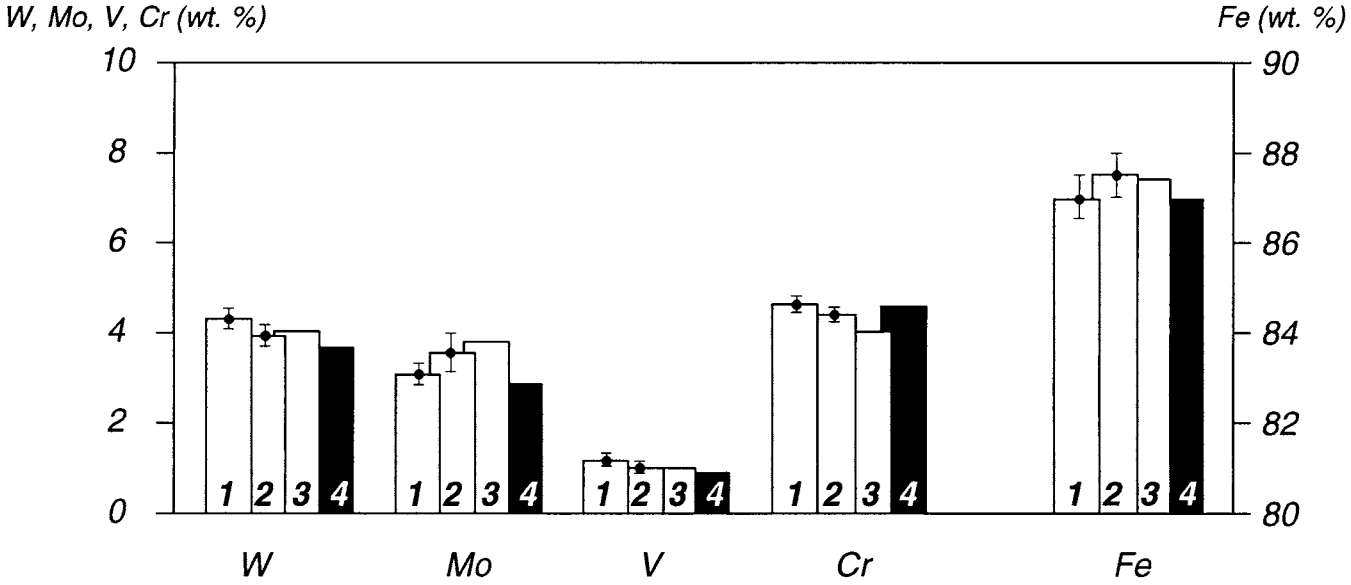

Fig. 1—Matrix composition of AISI M2 determined by different methods: (1) indirect—total alloy composition minus alloy elements fixed in blocky carbides (determined by quantitative metallography and carbide analysis by SEM/EDX); (2) STEM/EDX; (3) extraction analysis (data from Kim *et al.*[11]); and (4) Thermo-Calc calculation for austenite at 1230 °C.

timet 500 image analyzer. Unetched specimens must be used to avoid distortion of the volume fractions.[45,46] Obtaining sufficient resolution and contrast for automatic phase differentiation and volume fraction measurement is not trivial. Suitable images can be obtained in the secondary electron mode with low primary beam energy.[46,47] In the present study, an acceleration voltage of 5 kV was used throughout, except for alloy no. 4, which required a still lower beam voltage and the use of a field emission cathode.[47] Ten fields of view were analyzed for each steel at magnification 2000 times for conventional grades and at 3000 times for powder metallurgy materials. The powder processed Nb alloys had to be analyzed at 6000 times owing to the fineness of their undissolved carbides. The total number of carbide particles included in the analysis was between 900 and 1300 for the conventional alloys and between 1800 and 2700 for the powder processed materials.

To estimate the potential amounts of tertiary precipitates, it is necessary to know the matrix composition of each steel in the quenched state. Customarily, such measurements are made in the scanning electron microscope, in regions free of coarse carbides, using energy-dispersive X-ray fluorescence (SEM/EDX). However, unseen carbide particles beneath the section plane but within the excitation volume may distort the results. Therefore, independent determinations were made by other methods: first, by calculating the alloy elements bound in the large carbides from their measured volume fractions and compositions, and subtracting these from the total alloy compositions;[13] then by EDX measurements on thin foil specimens in a scanning transmission electron microscope (STEM/EDX),[13] which also allowed the carbon content of the matrix to be measured directly by electron energy loss spectroscopy. For AISI M2, independent data from electrolytic carbide extraction are available in the literature.[11] Finally, matrix compositions

Table II. Volume Fractions of Blocky Carbides and Matrix Compositions of Alloys 1 through 13*

Alloy Number	Alloy Type	Carbide Fraction (Vol Pct)			Matrix Composition (At. Pct)					
		f_{MC}	f_{M2C}	f_{M6C}	C	W	Mo	V	Cr	Co
1	T1	trc	11.0	—	2.07	2.37	0.25	0.69	4.09	—
2	M2	1.1	5.7	—	2.82	0.93	1.94	0.85	3.99	—
3	M7	1.7	9.6	trc	1.59	0.12	2.61	0.20	3.46	—
4	M42	—	2.3	5.0	2.94	0.30	2.48	0.68	3.44	7.32
5	PM/M2mod.	8.4	2.9	—	1.93	0.96	1.42	0.51	3.49	—
6	PM/T15mod.	8.6	3.1	—	2.78	2.02	0.97	1.35	3.27	7.89
7	exp. Nb	5.4	—	—	3.06	0.56	1.68	1.37	4.59	—
8	exp. Nb + 3Co	5.4	—	—	2.94	0.63	1.84	1.33	4.60	3.46
9	exp. Nb + 5Co	5.4	—	—	2.94	0.63	1.73	1.40	4.81	5.24
10	exp. Nb + 8Co	5.4	—	—	2.85	0.60	1.64	1.24	4.49	7.95
11	T1-Mx	—	trc	—	2.12	2.29	0.33	0.78	4.57	—
12	M2-Mx	trc	trc	—	2.60	1.22	2.12	1.11	5.06	—
13	M7-Mx	trc	trc	—	2.43	0.34	2.68	1.13	4.31	—

*Matrix compositions refer to quenched austenite (*cf.* discussion in Section III–A).

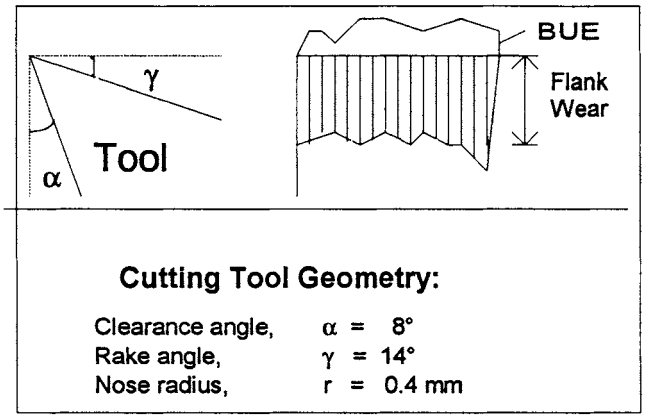

Fig. 2—Tool geometry and wear measurement on the flank. BUE = built-up edge.

were estimated by thermodynamical calculation using the Thermo-Calc procedure.[48] Very gratifying agreement is obtained between the various experiments and with the thermodynamics estimates (*cf.* Figure 1). This encourages us to accept the measurements shown in Table II as a serviceable basis for the correlation analysis.

C. *Tool Performance*

The performance of the various alloys was tested in continuous cutting. The work material was AISI O2, a cold work die steel of composition 0.9 pct C, 2.0 pct Mn, 0.35 pct Cr, and 0.13 pct V (wt pct). This material was annealed to a hardness of 200 HV10. Its high content of globular carbides makes it a very abrasive material to cut, and its soft ferrite produces intense adhesive wear. The tools were rectangular bars of 8 × 8 × 75 mm^3. Their ends were ground to the edge geometry specified in Figure 2. The depth of cut was 2.5 mm, and the feed rate was 0.19 mm/rev. A cutting fluid (Kutwell 40, Esso, Germany) was employed in all tests. Tool life measurements were replicated up to three times.

Three regimes of wear are generally encountered as the cutting speed is increased:[49,50] first, a built-up edge overlays the original tool geometry; then, as the built-up edge recedes, normal sliding wear is stabilized; finally, plastic blunting of the cutting edge becomes the dominating process. Preparatory tests showed that these regimes could be expected around 25, 35, and 45 m/min. These speeds were chosen for all alloys in order to examine each steel in each regime. This is important because high speed steels often see service under conditions of widely varying cutting speeds. The speeds were kept constant by adjusting the rotations per minute of the lathe as the work diameter decreased. To ensure comparability, the machinability of each new workpiece was calibrated using standardized reference tools.

Tool performance was characterized by the time to total blunting at each speed. This reflects the maximum usable tool life, bringing out the full effect of tertiary precipitates. In industrial practice, tools are terminated at a set fraction of their maximum life in the interest of safety and uniform surface quality.

Since high speed steels are often used with wear-reducing coatings, some alloys were tested with PVD TiN coatings[51] of 4 μm thickness. The effects of coating on the wear behavior of high speed steels have been described in the literature,[52,53,54] and our own observations on the present tool/coating/work combination have been published.[33]

III. RESULTS

A. *Microstructures*

Figures 3 and 4 show the microstructures of the steels in the finished, heat-treated, and tempered state. At these magnifications, only the undissolved carbides are seen. Their volume fraction is determined by the extent of dissolution during austenitization and is frozen during quenching. Table II shows the volume fractions of undissolved carbides and the matrix compositions of the steels. The ''matrix'' to which the measurements refer is the matter found between the undissolved carbides. The precipitates cannot be resolved and independently analyzed by the analytical methods employed (with the exception of APFIM[21,22,26]). Thus, the matrix compositions stated include the precipitate contents, giving, in effect, the composition of the quenched austenite, or the martensite before the onset of the precip-

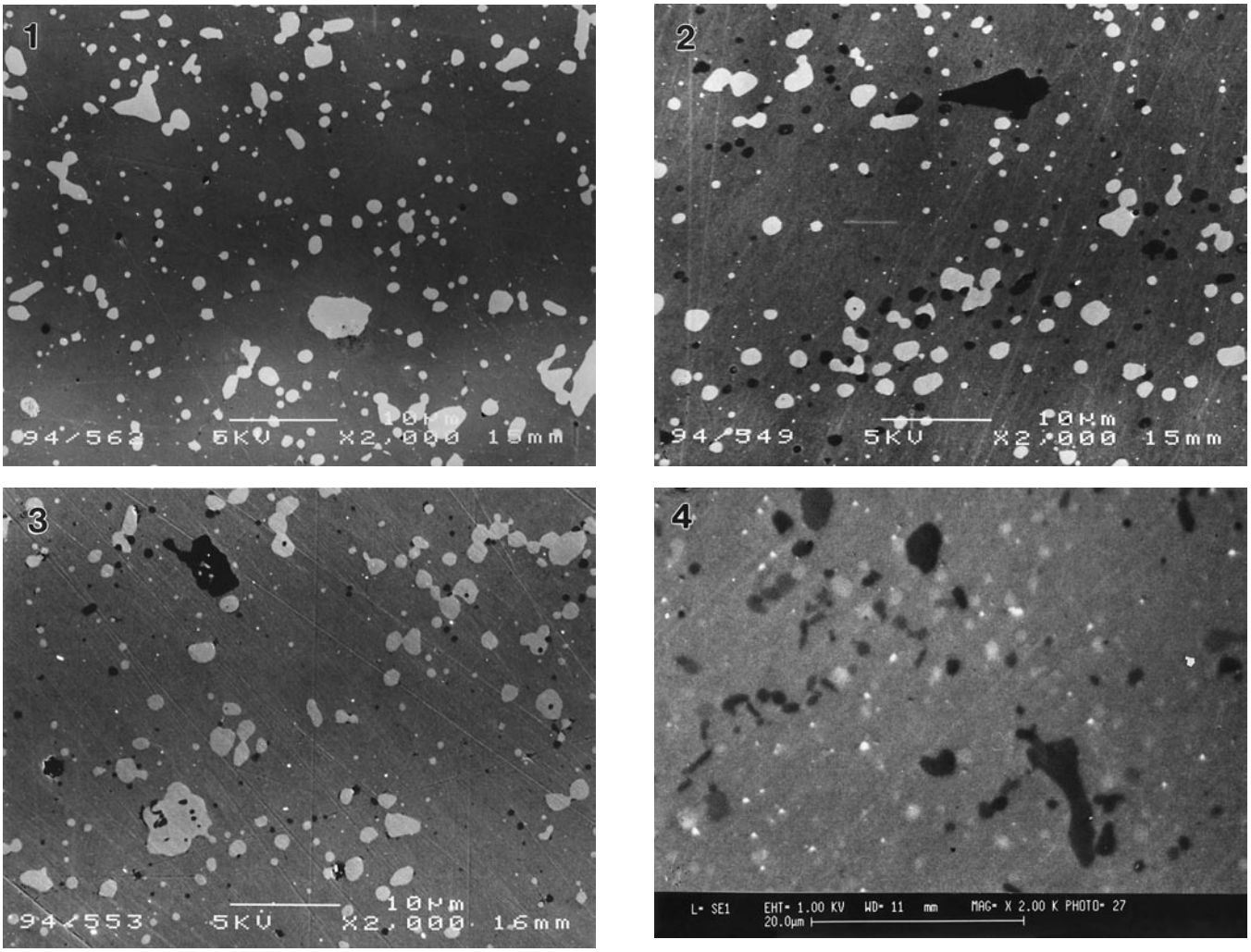

Fig. 3—Microstructures of alloys 1 through 4 (alloy number shown at left top) as used for image analysis (quenched and tempered state); scanning electron micrographs of unetched specimens in secondary electron mode. Light phase: M_6C (M_2C in 1); dark phase: MC.

itation reaction. Since our interest is directed at the driving force for the formation of precipitates, this is the quantity desired.

The relative amounts of ''primary'' MC, M_2C, and M_6C are determined by the alloy composition and the rate at which the material solidified from the melt.[55–58] M_6C contains large amounts of the weak carbide former Fe and is easily dissolved during austenitization. The opposite is true for MC. M_2C is a metastable carbide[58,59] which forms in most alloys during solidification but is usually decomposed during hot working and high annealing.[60,61,62] Thermodynamical calculations show that the nucleation of this carbide from the melt is due to enrichment of Mo and V in the undercooled interdendritic melt.[63] Molybdenum is a strong stabilizer of M_2C.[59] Therefore, it is not surprising that this phase survives best in the Mo-rich steels, M7 and M42.

The powder processed steels (Figure 4) show the expected absence of carbide stringers and the fine carbide particle size characteristic for this production route. The resultant toughness benefit is used to introduce larger amounts of MC (*cf.* Table II, alloy nos. 5 and 6). Also, in the experimental Nb alloys, powder processing has kept the NbC particles extremely small.

The secondary precipitates can be analyzed only by APFIM. They are of two types: MC and M_2C.[20,21] The precipitate volume fractions that have formed during tempering, and the maximum amounts of tertiary precipitates that could be formed during subsequent operation, are listed in Table III, based on APFIM measurements on alloys nos. 11, 12, 13, and 7.[22] The first three represent the matrices of T1, M2, and M7, respectively. The APFIM measurements yield the compositions of the M_2C and MC precipitates and their number ratio; in addition, APFIM gives the composition of the actual matrix between the secondary precipitates, in contrast to the global matrix compositions determined by the low resolution methods and shown in Table II. The difference between these values and the APFIM results shows the depletion of the matrix by the precipitate formation. When the number ratio MC:M_2C and the precipitate compositions are considered as constant through the secondary and tertiary stage, the total amount of precipitates can be calculated from this depletion. The number ratio MC:M_2C was found to be constant when different fields of view were examined in the field ion microscope.

The solutes left in the matrix at the end of the tempering treatment can form tertiary precipitates during tool operation, typically at temperatures of the order of 650 °C.[26]

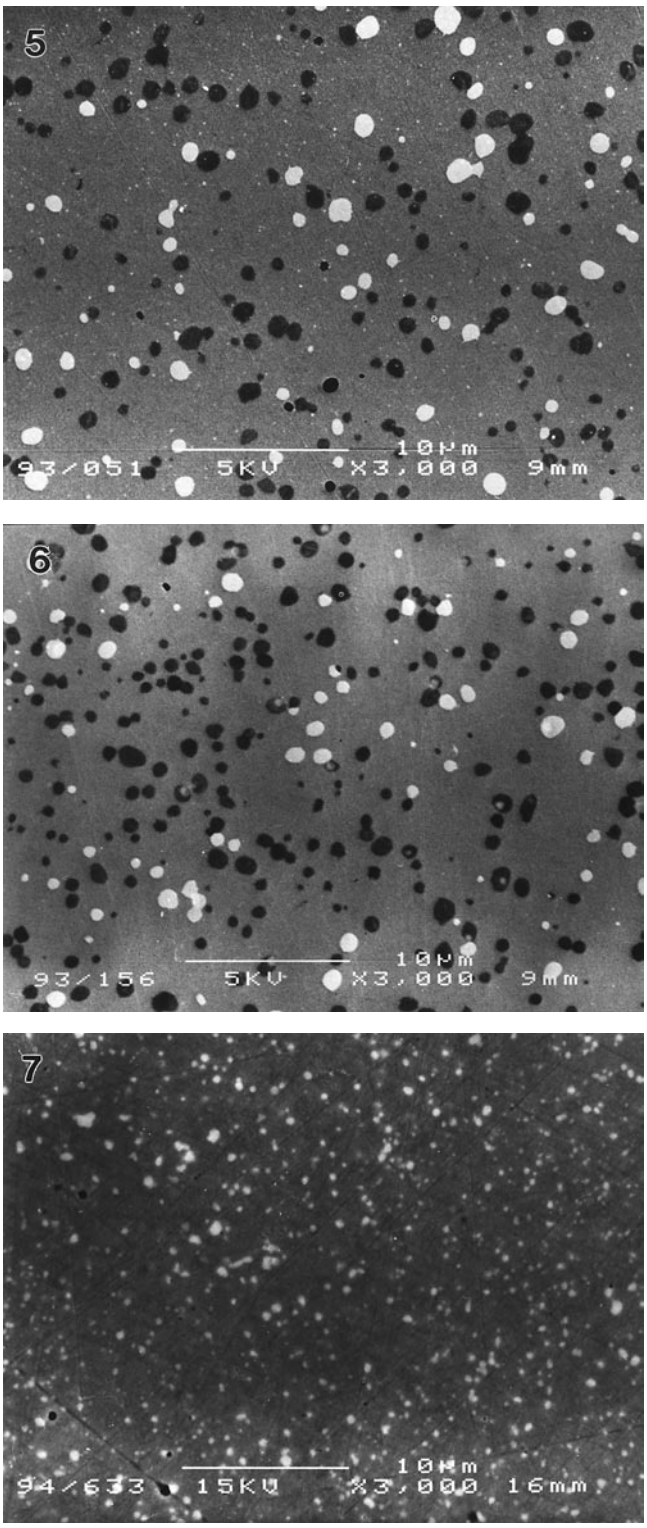

Fig. 4—Microstructures of alloys 5 through 7 (Fig. 3).

Precipitation can only proceed as long as sufficient carbon is available. Assuming (as the simplest hypothesis) that the ratio MC:M_2C and the phase compositions are the same in the tertiary reaction as during the original tempering, the maximum amount of tertiary precipitates and the contents of W, Cr, V, and Mo remaining in the matrix after the tertiary reaction can be calculated.

For alloy nos. 4 through 6, which were not analyzed by APFIM, the maximum possible precipitate formation was estimated as follows: APFIM work had shown a well-defined, linear correlation between matrix and carbide levels of Mo and W,[22] indicating constant partition ratios. The same ratios were adopted for the compositions of the secondary precipitates in the other alloys. With these compositions known, it is possible to calculate the maximum possible amounts of tertiary precipitation and the residual solute levels.

Since the model that forms the object of this study is directed at the maximum possible tool life, the proper quantity to characterize the strengthening effect of the precipitates is the sum of the secondary and the maximum possible tertiary precipitates. This quantity reflects the potential of the alloy to uphold sufficient hot strength during tool operation. In forerunners of the present work,[38,64] we have referred to this as matrix strengthening potential or matrix potential for short.

B. *Cutting Tests*

The development of wear during a cutting test is illustrated in Figure 5 for the case of alloy no. 2. Monitoring the flank wear (*cf.*, Figure 2) as a function of time (Figure 6), one finds three stages: (1) intense initial wear, followed by (2) a period of constant wear rate and finally by (3) catastrophic wear.

The cutting performance of tool materials is usually characterized by Taylor diagrams, relating the life (L) to the cutting speed (v) in log-log coordinates according to Taylor's formula:[65]

$$L = \text{const. } v^{-m} \qquad [1]$$

where m is a constant as long as the wear mechanism remains the same. Figure 7 shows data from our tests on AISI M2 (no. 2) as an example. Similar plots were made for all alloys tested, including the TiN-coated tools. The steep decline of the Taylor line at the highest cutting speed reflects the transition to plastic blunting as the decisive failure mechanism.

Figure 8 illustrates the effect of cutting speed on tool life for three popular alloys. The superiority of the cobalt-alloyed, carbide-enhanced PM grade T15 over the classical alloys M2 and M7 is clearly seen, especially at high speeds.

The effect of cobalt is the subject of Figure 9. The alloy base in this case is an experimental material containing Nb in partial exchange for V, but similar behavior is expected for conventional steels. As in the case of T15, the beneficial effect of Co is most prominent at the highest speed.

Figure 10 compares the performance of the carbide-free materials (nos. 12 and 13) to that of their carbide-containing parent alloys. At the lowest speed, the absence of the undissolved carbides has almost no effect. The built-up edge virtually precludes contact between tool and work. At the intermediate speed, where the tool is directly exposed to the abrasive work material, the blocky carbides have a distinctly beneficial effect. This seems to decrease again at the highest speed. Arguments in Section IV will point to a changeover from abrasion to thermal softening of the matrix at this speed.

Figure 10 also illustrates the effect of TiN coating for the case of M2 at intermediate speed. If the coating did completely assume the role of protecting the substrate from

Table III. Matrix Strengthening Potential (Volume Fraction of Precipitates Formed during Secondary Hardening, Extent of Possible Tertiary Precipitation during Tool Operation, and Residual Solute Content)

Alloy Number	Alloy Type	Matrix Precipitation (Vol Pct)					Residual Solute Content (At. Pct)			
		f^{sec}_{M2C}	f^{sec}_{MC}	f^{tert}_{M2C}	f^{tert}_{MC}	$\Sigma f^{sec+tert}_{carbide}$	W	Mo	V	Cr
1	T1	1.40	2.10	0.35	0.53	4.38	2.13	—	—	2.56
2	M2	2.10	0.90	2.56	1.10	6.66	0.64	—	—	2.92
3	M7	2.04	0.51	2.04	0.51	5.10	0.03	0.71	—	2.46
4	M42	3.30	0.83	3.30	0.83	8.26	0.17	—	—	1.84
5	PM/M2mod.	1.41	0.60	1.73	0.74	4.48	0.76	—	—	2.77
6	PM/T15mod.	2.74	1.17	1.82	0.78	6.51	1.73	0.46	—	1.33
7	PM/exp Nb	1.89	1.26	2.83	1.89	7.87	0.18	—	0.49	2.49
8	PM/exp Nb + 3Co	1.81	1.21	2.71	1.81	7.54	0.27	0.28	0.48	2.56
9	PM/exp Nb + 5Co	1.81	1.21	2.71	1.81	7.54	0.28	0.17	0.55	2.77
10	PM/exp Nb + 8Co	1.74	1.16	2.60	1.73	7.23	0.25	0.14	0.43	2.54
11	T1-Mx	1.44	2.15	0.36	0.54	4.49	2.05	—	—	3.01
12	M2-Mx	1.95	0.84	2.39	1.02	6.20	0.94	0.42	0.27	4.07
13	M7-Mx	3.05	0.76	3.05	0.76	7.62	0.21	0.25	—	2.83

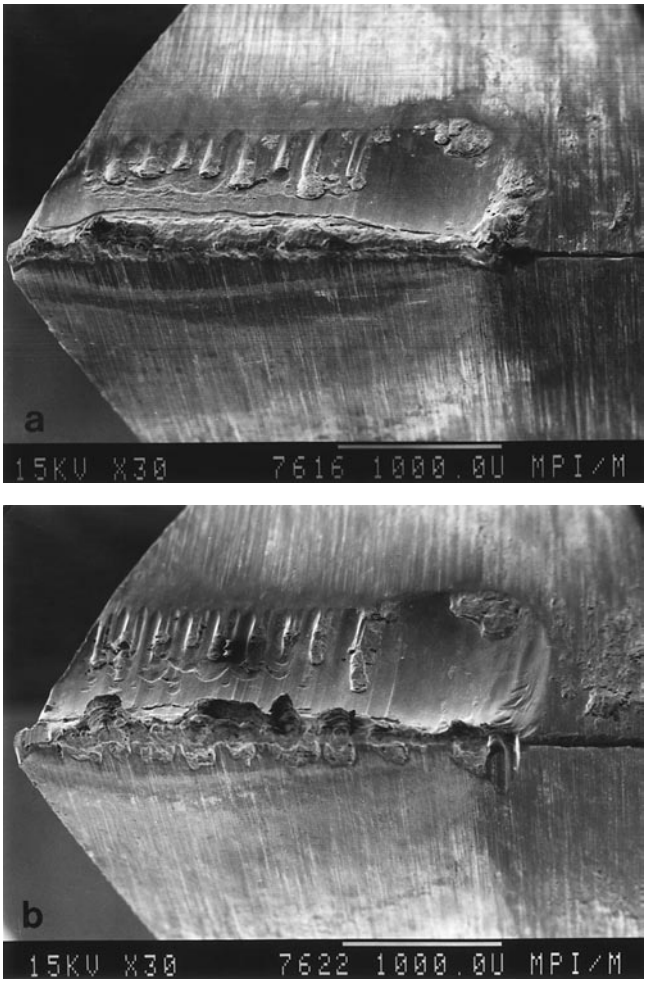

Fig. 5—Typical wear markings; alloy 6 (PM/T15mod.), v = 35 m/min: (*a*) 8.6 min and (*b*) 22.9 min.

abrasion, the difference between carbide-free and carbide-bearing substrates should vanish upon coating. This is not fully achieved. The remaining effect of the undissolved carbides may be attributed to a longer wear period after coating breakthrough.

Total tool lives in terms of minutes to total blunting are listed in Table IV.

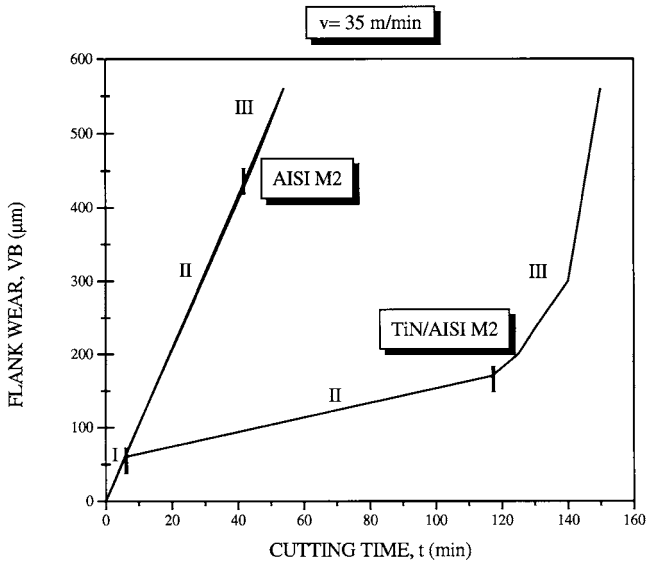

Fig. 6—Typical evolution of wear during a cutting test for alloy 2 (AISI M2), uncoated and coated with TiN.

IV. THE MODEL

The cutting tests presented in Figure 10 demonstrate that a strong matrix without support of blocky carbides generates appreciable tool life under conditions of predominantly thermal and mechanical loading (built-up edge regime and plastic blunting regime). In the intermediate speed regime, however, the blocky carbides contribute considerably to the life of the tool. A model for tool life prediction must therefore contain terms reflecting the role of both the undissolved carbides and the strengthening of the matrix, and we must expect the weight factors of these contributions to vary with the cutting speed.

The simplest hypothesis is that the contributions of the various factors to the total tool life are additive; present knowledge is not sufficiently detailed and reliable to justify more sophisticated assumptions. Consequently, the model is written as a linear combination of mechanism-related terms whose weight factors must be determined empirically:

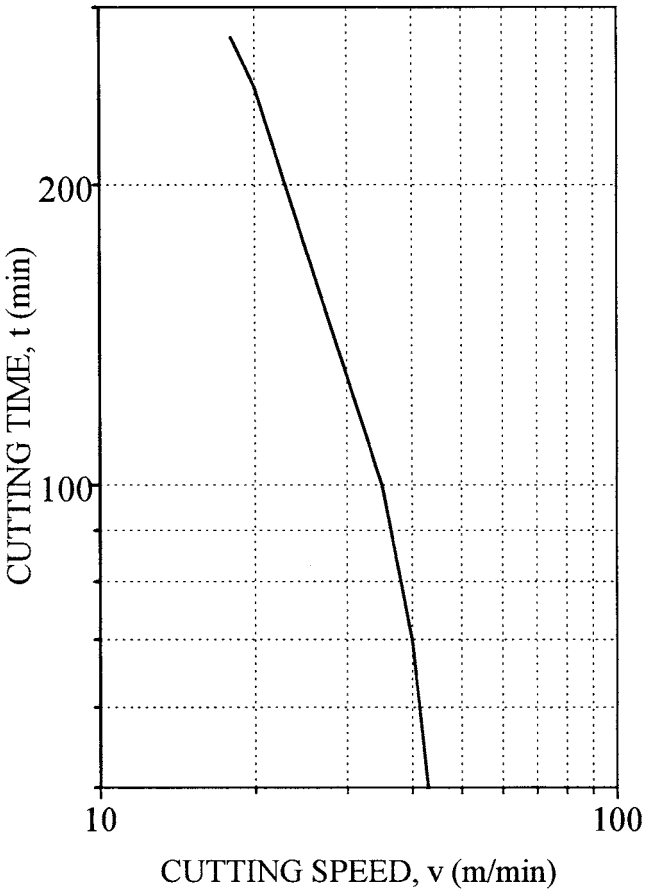

Fig. 7—Taylor plot for alloy 2 (AISI M2).

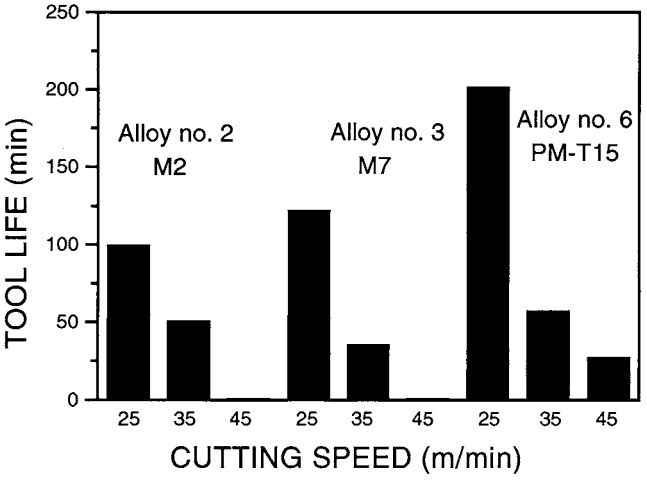

Fig. 8—Cutting test results for alloys 2 (AISI M2), 3 (AISI M7), and 6 (PM T15mod.).

$$L = b_1(f^{I}_{MC} + {}^{1}/_{2}f^{I}_{M2C}) + b_2 f^{I}_{M6C} + b_3 f^{II+III} + b_4 f^{II+III}[Co] + b_5([W] + [Mo] + [V])^{1/2} \quad [2]$$

In Eq. [2], the b's signify weight factors and the f's volume fractions. The superscripts mark the carbide generation: I for the primary (undissolved) carbides, and II + III for the secondary plus tertiary precipitates. Subscripts mark the carbide phase. For the undissolved carbides, a linear effect of volume fraction is suggested by the experience summarized in Section I.[24,27–29,35] Since only one alloy among

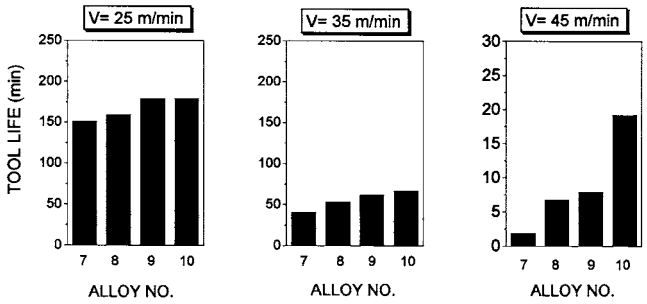

Fig. 9—The effect of Co on tool life: test results for Nb-bearing alloys with varying Co content. Note expansion of ordinate scale for v = 45 m/min.

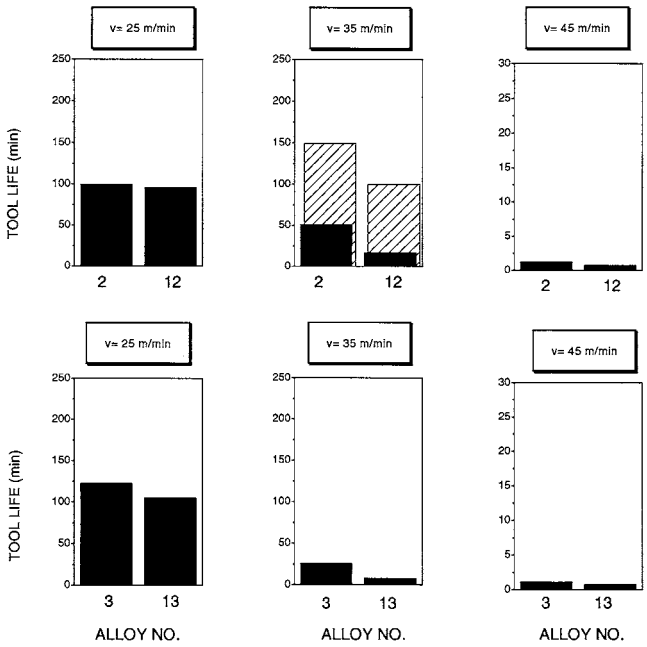

Fig. 10—Tool lives of carbide-free materials as compared with their carbide-containing parent alloys. Shaded bars in the top middle diagram are for TiN coated tools. Ordinate scale expanded for v = 45 m/min.

the 13 shows appreciable amounts of M_2C, the weight factor of this carbide cannot be meaningfully determined by regression analysis, and it was decided to lump this carbide with the MC phase. Somewhat arbitrarily, the weight factor for M_2C was fixed at one-half of that for MC in view of its lesser stability.

The strengthening effect of the precipitates at their most efficient size should be proportional to their volume fraction, and the known relation between tool life and tempered hardness[24,29,35,39] supports the choice of a linear relation. Since we are trying to model the maximum possible tool life (up to failure by blunting), we let the sum of the secondary and tertiary precipitates reflect the effect of matrix strengthening.

Element symbols in square brackets in Eq. [2], *e.g.*, [Co], signify the content of the element in atomic percent in the matrix after secondary and tertiary precipitation. Cobalt enters neither the undissolved carbides nor the secondary and tertiary precipitates.[21] We adopt the view that it acts by delaying precipitate coarsening, and perhaps also by enhancing precipitate nucleation, creating a finer precipitate dispersion. Consequently, the Co term is constructed in

Table IV. Measured Performances of the Steels Tested in This Study

Alloy Number	Alloy Type	Performance, L (min) L_1 (25 m/min)	L_2 (35 m/min)	L_3 (45 m/min)
1	T1	104.4	47.1	0.36
2	M2	99.4	50.9	1.24
3	M7	122.3	35.5	1.10
4	M42	97.2	50.9	1.78
5	PM/M2mod.	154.5	59.1	1.18
6	PM/T15mod.	201.7	57.5	27.27
7	PM/exp Nb	150.7	40.4	1.84
8	PM/exp Nb + 3Co	158.9	53.1	6.75
9	PM/exp Nb + 5Co	178.3	61.6	7.91
10	PM/exp Nb + 8Co	179.0	66.6	19.11
11	T1-Mx	93.4	0.5	0.16
12	M2-Mx	95.6	16.6	0.73
13	M7-Mx	104.8	7.4	0.72

Table V. Weight Coefficients of the Mechanisms That Cooperate in Determining Tool Life*

v (m/min)	b_1 (MC)	b_2 (M_6C, M_2C)	b_3 (Precipitate)	b_4 (Cobalt)	b_5 (Solute)	Δ_{RMS} (RMS Residue)
25	9.82	1.20	9.42	0.19	34.7	2.62
35	3.97	2.63	2.76	0.28	0	2.65
45	1.03	1.03	0.18	0.16	0	2.42

*Δ_{RMS} = root-mean-square of the residual differences, $(\Sigma\Delta^2)^{1/2}$.

such a way that it enhances the contribution of the precipitates.

The last term in Eq. [2] reflects the strengthening action of the residual solute after complete precipitate formation. The square-root dependence is modeled on Fleischer's theory of solute strengthening.[66,67] Differences in the strengthening efficiency of V, Mo, and W are neglected in the present coarse shape of the model.

Multiple linear regression analysis of the data listed in Tables II through IV yields the coefficients b_1 through b_5 shown in Table V.

Tool life tests notoriously show large scatter.[29,49,50] We estimate the probable error of our tool lives to be of the order of at least ± 5 minutes, possibly twice as much. Therefore, all tool lives below 5 minutes were omitted from the regression analysis. In the data for cutting speed 35 m/min, this concerns only one alloy (the carbide-free variant no. 11), but at 45 m/min, only the Co alloyed, powder processed grade nos. 6, 8, 9, and 10 remain as probably significant. This is insufficient for a regression analysis involving five coefficients, and therefore, the coefficients for the 45 m/min series were fixed by trial and error. Consequently, the 45 m/min measurements bring no added substance to the formulation and verification of the model, but it is gratifying to see that the weight factors obtained fit smoothly into the overall temperature dependence, as will be shown in Section IV (Figure 13).

Some 20 variants of Eq. [2] were tried for the regression analysis, searching for simpler models or, conversely, for terms that might have been missed. For instance, a purely additive term was tried for the effect of Co instead of the multiplicative coupling with the precipitate contribution, but it produced much poorer agreement between measured and calculated tool lives. Another avenue pursued was to test various ways of lumping all carbide phases together at fixed weight ratios chosen on the basis of considerations such as the hardness ratios. This approach was invited by the difficulty of accurate volume fraction measurements for the blocky carbide particles. Again, the fit was distinctly poorer for all the modified models than for Eq. [2] in the form shown. Many variants ruled themselves out by producing negative coefficients, which are physically meaningless. For instance, negative coefficients were obtained whenever the solute strengthening term b_5 was omitted, forcing us to admit this term in spite of initial doubts about its viability.

At the end of an extensive phase of variant testing, we felt satisfied that the quality of the fit is sensitive enough to changes in the correlation formula to conclude that the model described by Eq. [2] contains no unnecessary terms and that no terms of major importance are missing. On the other hand, each of the terms is justified by a distinct physical mechanism. Figure 11 shows that the correlation is quite close, and the absolute magnitudes of the deviations appear reasonable in light of typical error margins.

IV. DISCUSSION

The model behind Eq. [2] is based on known and relevant damage mechanisms in cutting tools. That such a simple model can describe the dependence of tool life on microstructural and chemical parameters over a range of almost 1:6, and for such widely different tool materials, is viewed as an important achievement and as support for principal adequacy of the underlying concepts.

Figure 12 shows, for each alloy, the contributions to the total tool life, which come from undissolved carbides, precipitates, cobalt, and solute strengthening. Figure 13 shows their variation with cutting speed, reflecting the changes in operating wear mechanisms with tool temperature.

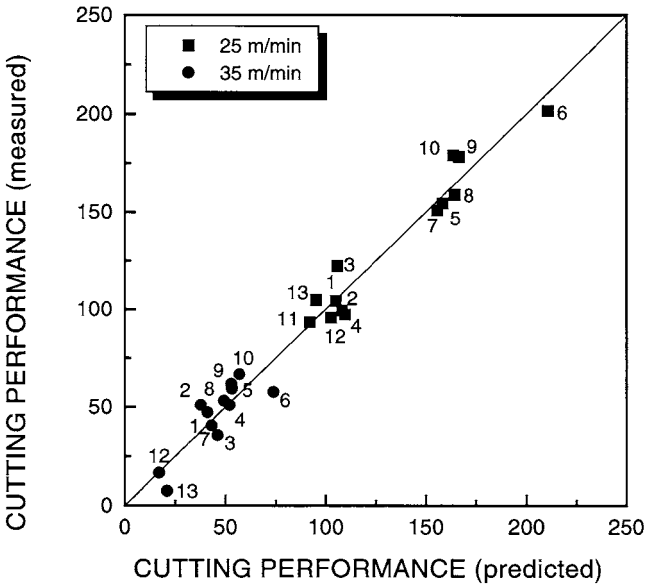

Fig. 11—Predicted *vs* measured tool lives.

Notable features are as follows.

(1) At the lowest cutting speed, the strongest contribution comes from matrix strength, but an independent contribution of the undissolved carbides cannot be neglected. It ranges from 5 pct in alloy no. 1 (AISI T1) to 50 pct in alloy no. 5, the powder processed, carbide enhanced variant of AISI M2. The primary carbide contribution becomes much more important at the intermediate speed, where the tool edge is not protected from abrasion. Here, it ranges from 70 pct in alloy nos. 1 and 3 (T1 and M7), and 76 pct in powder processed M2, to between 30 and 50 pct for the remainder. For those alloys that can be followed through the entire range of cutting speeds, Figure 13 confirms the preponderant importance of the blocky carbides at intermediate and high cutting speeds.

(2) Conversely, matrix strengthening by precipitates and solutes is important in the built-up edge regime, but its contribution diminishes at higher speeds, where the precipitates are bound to coarsen rapidly. The enhancement of the precipitate contribution by cobalt is of similar order at the two lower speeds. At the highest speed, where the precipitates quickly lose their effect in cobalt-free materials, the enhancement and stabilization of the precipitate effect by cobalt become highly important.

(3) Solute strengthening of the matrix by the alloy elements which remain in solution when tertiary precipitation has run to its end, appears surprisingly substantial at the lowest cutting speed, but seems to lose its importance completely at the higher speeds. One might speculate that at moderate temperatures, the solute atoms immobilize the dislocations in the martensite, while at the higher speeds and tool temperatures, they may lose some of their efficiency by increased mobility and possibly by clustering. At the moment, this explanation is purely speculative, and the matter would merit further investigation.

(4) The present results confirm the thesis, derived from earlier, less exhaustive observations,[38,64] that neither the secondary hardening of the matrix nor the volume fraction of undissolved carbides can account, taken by themselves, for the ranking of the alloys with respect to total cutting life. The potential of the matrix for continued precipitation, and the further contributions associated with residual solute content and with the enhancement of the precipitate effect by cobalt, must be taken into account. Consideration of Figure 12 will show that similar tool lives can be obtained with quite different levels of undissolved carbides, or of matrix potential. Obviously, the two contributions can substitute for each other within certain limits. Both must be considered if one wants to account correctly for the ranking of tool lives.

(5) The additive structure of our model is supported by comparing alloys 1 through 3 in Figures 12(a) and (b) with their carbide-free counterparts, nos. 11 through 13: keeping in mind the error margins of the experimental

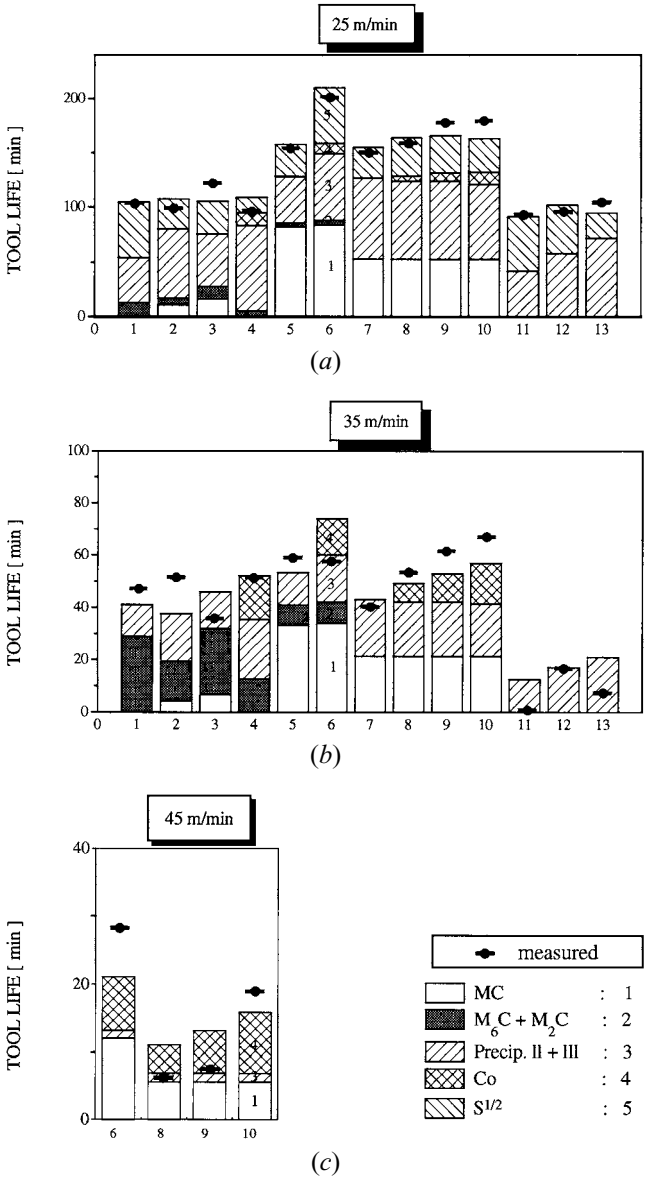

Fig. 12—Microstructural contributions to predicted tool lives (note different ordinate scales): (*a*) for 25 m/min, (*b*) for 35 m/min, and (*c*) for 45 m/min.

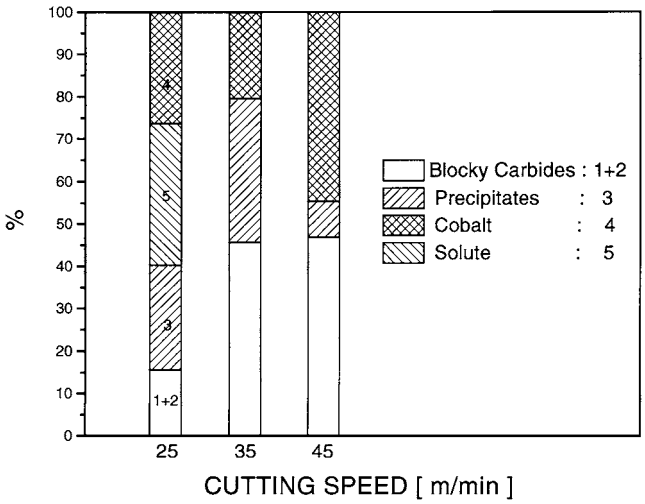

Fig. 13—Variation of the relative contributions of the microstructural parameters to tool life with cutting speed (averages of terms shown in Figs. 12(a) through (c) for alloys 6, 8, 9, and 10).

data, the fractions of total tool life that have been identified as contributions of the matrix (including solute effects) in the carbide-bearing alloys are quite similar in magnitude to the total lives of the carbide-free alloys.

(6) The effect of cobalt seems to be correctly represented as an enhancement of existing precipitate strengthening. The weight factor associated with this (b_4) may, in fact, have been underestimated by the regression analysis owing to an unlucky combination of errors in the experimental database. Considering the series of alloy nos. 7 to 10, which has increasing Co content with a constant base composition, the Co coefficient given in Table V clearly under-represents the Co effect. The value of b_4 is pulled down by the tool lives of alloy nos. 4 and 6, in which large contributions from other mechanisms leave little room for a Co contribution. Assuming that the tool lives of these alloys might have been accidentally shortened by causes such as early local damage to the cutting edge, we tested how much the Co coefficient might be increased. It turned out that without seriously impairing the overall fit as reflected by the root-mean-square residue, b_4 could actually be doubled before significant changes in the other coefficients became necessary.

To put the agreement of calculated and measured tool lives into proper perspective, it should be recalled in considering Figure 12 that the error band of the tool life measurements is possibly as wide as ± 10 minutes. The errors associated with the determination of carbide volume fractions and with the chemical composition of the matrix[45] compound to a similar magnitude in the calculated tool lives. In this light, the residual differences between measured tool lives and the values predicted by the model appear insignificant, and the model may be said to work satisfactorily. On the other hand, the verification of the model by comparison with experimental data looses some of its convincing power if this ''softness'' of the database is duly appreciated. Nevertheless, we feel that the model presented here appears sufficiently legitimatized to supply guidelines for alloy development by assigning discrete numbers to the relative importance of the contributions from undissolved carbide and matrix strengthening potential, and by supplying quantitative indications to the dominant wear mechanisms at the various cutting speeds.

The variation of the coefficients b_1 through b_5, which is detailed in Table V and illustrated in Figure 13, tells us that for uninterrupted cutting at low speed, the contribution of the undissolved carbides is secondary to that of matrix strengthening by precipitates and solutes. As suggested previously, the likely explanation is that the tool edge is protected from abrasion by the built-up edge. At higher cutting speeds, the built-up edge recedes, and direct contact between tool and chip admits both adhesive and abrasive wear. Under these conditions, the undissolved carbides become important. The higher tool temperature also increases the importance of delaying precipitate coarsening by cobalt.

Note that the tertiary precipitates, which have come to be considered only quite recently,[26,64] turn out to play an appreciable role at intermediate cutting speeds. While their contributions are not shown separately in Figures 12 and 13, they can be appreciated from the data in Table III. As much as 20 to 60 pct of the total precipitate population belong to the tertiary group. Similarly, the contribution of solute strengthening, which had not been considered at all in earlier discussions, is found to be highly important at tool temperatures low enough to keep the solutes attached to the dislocations.

Despite the widespread use of hard coatings on high speed steels, the properties of the substrate steel have not become inessential. As shown elsewhere,[33] direct contact between the tool material and the chip occurs early at the flank and somewhat later in the small breakaway region on the crater face. The growth of the crater, although generally delayed by the more favorable chip flow and friction conditions due to the coating, is largely controlled by the wear resistance of the substrate itself, and the flank wear is simultaneously affected by the shift of the site of maximum plastic work density as the crater geometry changes.

Finally, let us emphasize the limitations of the present work. It can point the way for applications of the model, but it cannot supply the specific coefficients to adapt it to all relevant service conditions. The present article deals exclusively with uninterrupted cutting in one single work material. For other work materials, the coefficients will have to be determined anew. This implies essentially a duplication of the regression analysis described here with tool life data for the new work material. (The microstructural characteristics of the tool alloys might be taken from the present work if their compositions were sufficiently similar to ours.) Such transfer of the modeling procedure to other work/tool combinations would eventually produce detailed and quantified insight into the action of the various wear mechanisms under given cutting conditions, which could serve as a basis for alloy optimization on a more sophisticated level than hitherto.

For interrupted cutting, the situation appears less hopeful to us. Present knowledge about the development of edge damage during interrupted cutting may not be sufficiently detailed and reliable to develop the additional components of the model, though the underlying principle should be applicable to interrupted cutting as well. Additional terms would be required to account for the defect population, following existing concepts.[8] The poor present state of knowl-

edge about crack growth rates under thermomechanical fatigue in high speed steels appears to be the greatest hurdle to such an extension of the model to interrupted cutting, unless one were to resort to a largely parametric treatment.

ACKNOWLEDGMENTS

One of the authors (SK) gratefully acknowledges the support of the Alexander von Humboldt Foundation during his work at the Max-Planck-Institut. Both authors acknowledge valuable assistance with quantitative metallography from Mr. H. Opielka, with statistical evaluations from Dr. T. Steinkopff, and with tool life tests from Messrs. H. Eckstein and W. Rösch. Large amounts of heat-treated work material and the tool materials themselves were placed at our disposal by Böhler-Uddeholm (Kapfenberg, Austria) through the good offices of Drs. G. Hackl, B. Hribernik, and H. Jäger.

REFERENCES

1. G. Hoyle: *High Speed Steels*, Butterworth and Co., Cambridge, United Kingdom, 1988.
2. G.A. Roberts: *Trans. AIME*, 1966, vol. 236, pp. 950-63.
3. R. Riedl, S. Karagöz, H.F. Fischmeister, and F. Jeglitsch: *Steel Res.*, 1987, vol. 58, pp. 339-52.
4. H.F. Fischmeister and L. Olsson: *Cutting Tool Materials*, ASM, Metals Park, OH, 1981, pp. 111-31.
5. H.F. Fischmeister: *Specialty Steels and Hard Materials*, IUPAP Conf, Pretoria, N.R. Comins and J.B. Clark, eds., Pergamon Press, Oxford, United Kingdom, 1983, pp. 127-40.
6. S. Karagöz and H.F. Fischmeister: *Steel Res.*, 1987, vol. 58, pp. 353-61.
7. E.A. Almond: *Specialty Steels and Hard Materials*, IUPAP Conf., Pretoria, N.R. Comins and J.B. Clark, eds., Pergamon Press, Oxford, United Kingdom, 1983, pp. 353-60.
8. H.F. Fischmeister, J. Paul, and S. Karagöz: *Pract. Metallogr.*, 1988, vol. 25, pp. 28-40.
9. A.R. Johnson: *Metall. Trans. A*, 1977, vol. 8A, pp. 891-97.
10. F. Kayser and M. Cohen: *Met. Progr.*, 1952, vol. 61, pp. 79-85.
11. C. Kim, V. Biss, and W.F. Hosford: *Metall. Trans. A*, 1982, vol. 13A, pp. 185-91.
12. S.C. Lee and F.J. Worzala: *Metall. Trans. A*, 1981, vol. 12A, pp. 1477-84.
13. S. Karagöz, I. Liem, E. Bischoff, and H.F. Fischmeister: *Metall. Trans. A*, 1989, vol. 20A, pp. 2695-2701.
14. K. Kuo: *J. Iron Steel Inst.*, 1953, vol. 174, pp. 223-28.
15. K. Kuo: *J. Iron Steel Inst.*, 1956, vol. 184, pp. 258-68.
16. P. Payson: *Trans. ASM*, 1959, vol. 51, pp. 60-93.
17. R.W.K. Honeycombe: Special Report 86, Iron and Steel Institute, London, 1964.
18. A.T. Davenport and R.W.K. Honeycombe: *Met. Sci.*, 1975, vol. 9, pp. 201-08.
19. R.J. Tunney and N. Ridley: *Met. Sci.*, 1978, vol. 12, pp. 585-90.
20. H.O. Andrén: *Scripta Metall.*, 1981, vol. 15, pp. 749-52.
21. K. Stiller, L.E. Svensson, P.R. Howell, W. Rong, H.O. Andrén, and G.L. Dunlop: *Acta Metall.*, 1984, vol. 32, pp. 1457-67.
22. H.F. Fischmeister, S. Karagöz, and H.O. Andrèn: *Acta Metall.*, 1988, vol. 36, pp. 817-25.
23. W.E. Henderer: *J. Eng. Mater. Technol.*, 1992, vol. 114, pp. 459-64.
24. A.M. El-Rakayby and B. Mills: *Wear*, 1986, vol. 112, pp. 327-40.
25. S. Söderberg: *Fagersta High Speed Steel Symp.*, September 1981, pp. 44-57.
26. H.F. Fischmeister, S. Karagöz, H.O. Andrén, and C.G. Jun: *Metall. Trans. A*, 1992, vol. 23A, pp. 1631-40.
27. P.K. Wright and E.M. Trent: *Met. Technol.*, 1974, vol. 1, pp. 13-23.
28. S. Söderberg, S. Hogmark, H. Haag, and H. Wisell: *Met. Technol.*, 1983, vol. 10, pp. 471-81.
29. S. Söderberg and S. Hogmark: *Wear*, 1986, vol. 110, pp. 315-29.
30. P.K. Wright, A. Bagchi, and J.G. Horne: *Cutting Tool Materials*, ASM, Metals Park, OH, 1981, pp. 7-23.
31. G. Vieregge: *Zerspanung der Eisenwerkstoffe*, 2nd ed., Verlag Stahl Eisen, Düsseldorf, 1970.
32. E.M. Trent: *Fagersta High Speed Steel Symp.*, September 1978, pp. 5-14.
33. S. Karagöz and H.F. Fischmeister: *Surf. Coat. Technol.*, 1996, vol. 81, pp. 190-200.
34. P. Clayton: *Wear*, 1980, vol. 60, pp. 75-93.
35. S. Söderberg, O. Vingsbo, B. Loryd, and B. Fredriksson: *Met. Corr. Ind.*, 1981, vol. 57, pp. 169-83.
36. I.M. Hutchings: *Mater. Sci. Technol.*, 1994, vol. 10, pp. 513-17.
37. L. Åhman, S. Hogmark, H. Haag, and H. Wisell: *Scand. J. Metall.*, 1982, vol. 11, pp. 299-308.
38. H.F. Fischmeister, S. Karagöz, E. Kudielka, and J. Püber: *Proc. Coll. Aciers Speciaux*, St. Etienne, 1983, Circle d'Etudes des Mètaux, St. Etienne, 1983, paper no. 6.
39. W.E. Henderer: *J. Eng. Ind.*, 1979, vol. 101, pp. 217-22.
40. G. Steven, A.E. Nehrenberg, and T.V. Philip: *Trans. ASM*, 1964, vol. 57, pp. 925-48.
41. W. Crafts and J.L. Lamont: *Trans. AIME*, 1949, vol. 186, pp. 957-67.
42. P. Hellman: *Cutting Tool Materials*, ASM, Metals Park, OH, 1981, pp. 168-80.
43. S. Karagöz and H.F. Fischmeister: *Metall. Trans. A*, 1988, vol. 19A, pp. 1395-1401.
44. S.R. Keown, E. Kudielka, and F. Heisterkamp: *Met. Technol.*, 1980, vol. 7, pp. 50-57.
45. S. Karagöz, I. Liem, J. Paul, and M. Poech: *Proc. ESS IV-2*, Göteborg, 1985; *Acta Stereol.*, 1986, vol. 5/2, pp. 287-97.
46. S. Karagöz and H.F. Fischmeister: *Steel Res.*, 1987, vol. 58, pp. 46-51.
47. E. Bischoff, H. Opielka, I.J. Kabyemera, and S. Karagöz: *Pract. Metallogr.*, 1995, vol. 32, pp. 77-89.
48. J.A. Golczewski and H.F. Fischmeister: *Steel Res.*, 1992, vol. 63, pp. 354-60.
49. E.M. Trent: *Metal Cutting*, 2nd ed., Butterworth and Co., London, 1984.
50. W. König: *Fertigungsverfahren, Band 1*, VDI Verlag, Düsseldorf, 1990.
51. J. Vetter, W. Burgmer, and A.J. Perry: *Surf. Coat. Technol.*, 1993, vol. 59, pp. 152-55.
52. P. Hedenqvist, M. Olsson, P. Wallen, Å. Kassman, S. Hogmark, and S. Jacobson: *Surf. Coat. Technol.*, 1990, vol. 41, pp. 243-56.
53. B.H. El-Bialy, A.H. Redford, and B. Mills: *Surf. Eng.*, 1986, vol. 2, pp. 29-34.
54. G.R. Fenske, N. Kaufherr, R.H. Lee, B.M. Kramer, R.F. Bunshah, and W.D. Sproul: *Surf. Coat. Technol.*, 1988, vol. 36, pp. 791-800.
55. H.F. Fischmeister, R. Riedl, and S. Karagöz: *Metall. Trans. A*, 1989, vol. 20A, pp. 2133-48.
56. H. Fredriksson: *Met. Sci.*, 1976, vol. 10, pp. 77-86.
57. R.H. Barkalow, R.W. Kraft, and J.I. Goldstein: *Metall. Trans.*, 1972, vol. 3, pp. 919-26.
58. J.A. Golczewski and H.F. Fischmeister: *Z. Metallk.*, 1993, vol. 84, pp. 557-62.
59. R. Riedl, S. Karagöz, M.R. Gregg, and H.F. Fischmeister: *Pract. Metallogr., Sonderband 14*, 1983, pp. 369-82; *The Charles Hatchett Award Papers*, The Institute of Metals, London, and CBMM, Sao Paulo, 1986, pp. 15-19.
60. E. Horn: *DEW-Techn. Ber.*, 1972, vol. 12, pp. 217-24.
61. H. Fredriksson, M. Hillert, and M. Nica: *Scand. J. Metall.*, 1979, vol. 8, pp. 115-22.
62. S. Karagöz, K. Schur, and H.F. Fischmeister: *Beitr. Elektronenmikroskop. Direktabb. Oberfl.*, 1982, vol. 15, pp. 235-38.
63. J.A. Golczewski and H.F. Fischmeister: *Z. Metallkd.*, 1993, vol. 84, pp. 860-66.
64. S. Karagöz and H.F. Fischmeister: *1st High Speed Steel Conf.*, G. Hackl and B. Hribernik, eds., Klampfer GmbH, Weiz, Austria, 1991, pp. 41-51.
65. J. Taylor: *Int. J. Mach. Tool Des. Res.*, 1962, vol. 2, pp. 119-52.
66. R.L. Fleischer: *Acta Metall.*, 1961, vol. 9, pp. 996-1000.
67. P. Haasen: in *Physical Metallurgy, Part II*, 4th ed., R.W. Cahn and P. Haasen, eds., North-Holland Physics Publishing, Amsterdam, 1996.